García-Ballesteros, S.; Mora Carbonell, M.; Vicente Candela, R.; Vercher Pérez, RF.; Sabater Marco, C.; Castillo López, M.; Amat Payá, AM.... (2019). A new methodology to assess the performance of AOPs in complex samples: Application to the degradation of phenolic compounds by O3 and O3/UV-A Vis. Chemosphere. 222:114-123. https://doi.org/10.1016/j.chemosphere.2019.01.015

A new methodology to assess the performance of AOPs in complex samples: Application to the degradation of phenolic compounds by O_3 and O_3/UVA-vis

S. García-Ballesteros[a], M. Mora[b], R. Vicente[a], R.F.Vercher[a], C. Sabater[c], M.A. Castillo[c], A.M. Amat[a], A. Arques[a]

[a] Grupo de Procesos de Oxidación Avanzada, Departamento de Ingeniería Textil y Papelera, Universitat Politècnica de València, Campus de Alcoy, Alcoy, Spain.

[b] Grupo de Procesos de Oxidación Avanzada, Departamento de Matemática Aplicada, Universitat Politècnica de València, Campus de Alcoy, Alcoy, Spain.

[c] Dpto. Biotecnología. Universitat Politècnica de València. Camino de Vera, s/ n. 46022 – Valencia, Spain

Abstract

A methodology combining experimental design methodology, liquid chromatography, excitation emission matrixes (EEM) and bioassays has been applied to study the performance of O_3 and O_3/UVA-vis in the treatment of a mixture of eight phenolic pollutants. An experimental design methodology based on Doehlert matrixes was employed to determine the effect of pH (between 3 and 12), ozone dosage (02-1.0 g/h) and initial concentration of the pollutants (1-6 mg/L each). The following conclusions were obtained: a) acidic pH and low O_3 dosage resulted in an inefficient process, b) increasing pH and O_3 amount produced an enhancement of the reaction, and c)

interaction of basic pH and high amounts of ozone decreased the efficiency of the process. The combination of O_3/UVA-vis was able to enhance ozonation in those experimental regions were this reagent was less efficient, namely low pH and low ozone dosages. The application of EEM-PARAFAC showed four components, corresponding to the parent pollutants and three different groups of reaction product and its evolution with time. Bioassys indicated important detoxification (from 100% to less than 30% after 1 min of treatment with initial pollutant concentration of 6 mg/L, pH = 9 and ozone dosage of 0.8 g/h) according to the studied methods (*D. magna and P. subcapitata*). Also estrogenic activity and dioxin-like behavior were significantly decreased.

Keywords

Ozone, UV-VIS, phenolic compounds, Doehlert matrix, toxicity, excitation emission matrix fluorimetry

Graphical abstract

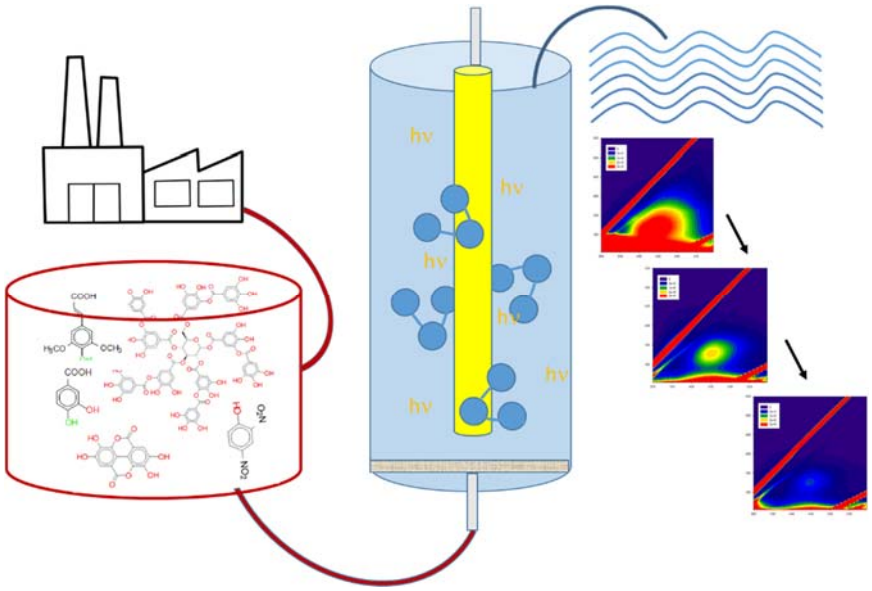

Highlights

- UV-A-vis light improves the efficiency of the ozonation at acid pH and low O_3 concentration.
- EEM is a good technique to detect intermediates in the oxidation process.
- PARAFAC is able to decompose the EEM into more simple components, allowing monitoring of the generated intermediates.
- This process resulted in a decrease in estrogenic and dioxine-like properties and detoxification (standard bioassays).

1. Introduction

Food processing industry (e.g. wine, olive mill or cork boiling) produces highly polluted effluents, containing sugars, tannins and (poly)phenolic compounds, among other substances at different concentrations. For instance, high concentrations of polyphenols

(ca. 1300 mg/L) can be found in the wastewater originated in the baking process of cork (Mendoça et al., 2004). Since some of those compounds are refractory to classical treatments, development of alternative techniques to deal with these effluents seems necessary. In this context, advanced oxidation processes (AOPs) have received great attention in the last two decades, and promising results have been obtained in most cases (Vilar et al., 2009).

One of the AOPs that have been considered is ozonation. This process does not only involve direct reaction of molecular ozone with the pollutant, but also an indirect mechanism involving hydroxyl radicals (Dodd et al, 2009; Beltran, 2003). The mechanism is pH dependent: while in acidic medium attack of molecular ozone is predominating, at basic pH decomposition of O_3 into highly reactive ·OH is favoured (Ikehata and El Din, 2004, Ikehata, 2006). These differences in the prevailing mechanism explains the higher efficiency of ozonation at high pH values (Luis et al, 2011): reaction with molecular ozone is selective towards some moieties such as double bonds or aromatic rings, while hydroxyl radicals are unselective and, in general, more reactive (Legrini et al, 1993). This pH dependence is even more evident in the case of mineralization of organic matter, that is a goal more difficult to be achieved due to the formation of by-products that, in turn, should be removed (Ribeiro et al, 2015); in fact, high pH is needed to reach significant mineralization of effluents (Beltran, 2003). Alternative ways to generate hydroxyl radicals from ozone is the combination of this gas with other substances such as TiO_2 (Rivas et al. 2012, Tichonovas et al., 2017), Fe(III) (Quiñones, 2015), zero-valent zinc (Zhang et al. 2015), hydrogen peroxide (Mizuno et al., 2011).

Also irradiation can be employed to generate ·OH from ozone (Kuo, 1999). In fact, decomposition of O_3 in water under UVC irradiation has been widely studied. The mechanism of the process is complex and depends on different parameters, such as the pH (Chávez, 2016), or the presence of radical scavengers in the reaction medium (Garoma, 2005). In general, UV irradiation and ozonation show an important synergetic effect, both in pollutants removal and in mineralization of the organics present in the effluent (Orge et al., 2017, Lovato et al., 2017), what is useful in the treatment of effluents having high concentration of organic matter (Collivignarelli et al., 2004). The higher efficiency of O_3/irradiation has been reported to reduce the amount of ozone that is required and hence, the energy consumption (Quiñones et al., 2015).

The UVA fraction can also be employed for this purpose, although the efficiency is lower than UVC, as the absorption of ozone in this interval is very low (see Oh et al., 2016 for the spectrum of ozone in aqueous solution) . However, this approach is interesting as sunlight can be employed as irradiation source (Marquez et al, 2014; Quiñones et al., 2015) and it has been reported to enhance the process in the conditions more disfavourable for ozonation, namely acidic pH (Chavez et al., 2016). In fact, recent studies have shown that irradiation results in an enhancement of the process efficiency, although the intensity of light has scarce influence on the oxidation rate (Siqueira and Amaral, 2015).

With this background, this work has two major goals that are: a) to study the use of O_3 and its combination with simulated sunlight in the removal of phenolic components commonly found in food processing effluents and b) to develop a reliable methodology

to monitor the performance of AOPs in complex samples. For this purpose, a mixture of six phenolic compounds (2,4-dinitrophenol, gallic acid, protecatechuic acid, vanillic acid, syringic acid and sinapic acid) and two polyphenols (tannic acid and elagic acid,) were chosen; this group of pollutants has already be employed to check the effect of photo-Fenton in these type of effluents (García Ballesteros el al., 2016). Ozonation was performed with and without irradiation with a xenon lamp under different conditions and experimental design methodology based on Doehlert matrices was used to determine the effect of experimental conditions (Ferreira et al., 2004); this methodology has been commonly employed for this purpose in wastewater treatment processes (Gomis et al., 2015). In order to follow the effect of ozonation on the mixture of phenolic compounds, excitation emission matrices (EEM) have been employed. This technique is based on the measurement of bi-dimensional plots in which the fluorescence emission spectra of the sample is plotted versus the wavelength of the excitation source (Chen et al., 2003). It provides interesting structural information on the organic matter present in solution and it increasingly used to analyse the behaviour of complex samples as it provides alternative information of fluorescent by-products to chromatography if the aim of the work is not to establish a detail degradation path has to be established. (Liu et al, 2015 and 2016).

In this work, parallel factor analysis (PARAFAC) has been employed to gain further insight into the information provided by EEM. This mathematical procedure allows decomposing the EEM into different components, which can be assigned to chromophores or groups of substances; hence, major trends in decomposition of pollutants in complex mixtures can be recognized (García-Ballesteros et al., 2016; Mangalgiri et al., 2017). Finally, a battery of bioassays have been employed to monitor detoxification of the solution along the treatment.

2. Experimental

2.1 Reagents, microorganisms and cell lines

2,4-dinitrophenol, tannic acid, elagic acid, gallic acid, protecatechuic acid, vanillic acid, syringic acid and sinapic acid were purchased from Sigma-Aldrich and used as received. Ultra-pure water (Mili-Q) was used to prepare all solutions.

P. *subcapitata* and *ephippia* (dormant eggs) of D. *magna*, employed for the bioassays were supplied by ECOtest S.L. (Valencia, Spain). Two recombinant strains of *Saccharomyces cerevisiae* were employed: BY4741 strain to detect estrogenic activity (ER strain) and YCM4 strain to monitor aryl hydrocarbon receptor agonist activity (AhR strain); they were kindly provided by Dr. Benjamin Piña from IDAEA-CSIC, Barcelona, Spain.

Medium constituents employed in bioassays were supplied by Difco (Basel, Switzerland). Prototrophic markers, standards (17- β-estradiol (E2) and β-naphthoflavone (β-NF)) and enzymatic substrate (4-methylumbelliferone β-D-galactopyranoside and β-mercaptoethanol) were purchased form Sigma-Aldrich. Assay buffer (Triton X-100) and Y-PER (Yeast Protein Extraction Reagent) were supplied by Fisher Chemical and Thermo Scientific, respectively.

2.2. Reaction conditions

Ozonation tests were performed in a cylindrical glass reactor with 1 L capacity which has been described elsewhere (Amat et al., 2003). Ozone was supplied by a generator (Ozogas, T.R.C.E. 4000), able to produce 8 g/h when fed with oxygen. The ozone

152 production was tuned to the desired experimental conditions, with a production between
153 0.2 and 1 g/h. UVA-vis irradiation tests were performed by means of a xenon lamp
154 (Heraeus TXE 150), which solar spectrum closely matches the solar one (see
155 http://peschl-ultraviolet.com for spectrum), which was placed axially inside the
156 cylindrical reactor. The lamp, which power was 220 W, was inside a Pyrex glass
157 envelope that cuts off radiation below 300 nm. The system was refrigerated by water. In
158 all cases, the reactor was loaded with 250 mL and the gas flow was 10 NL/min.

159

160 2.3. Chemical analysis

161 The concentration of the six pollutants with low molecular weight (2,4-dinitrophenol,
162 gallic acid, protecatechuic acid, vanillic acid, syringic acid and sinapic acid) was
163 determined by liquid chromatography (Perkin Elmer model Flexiar UPLC FX-10). A
164 Bronwnlee Analytical column (DB-C18) was employed as stationary phase. The eluent
165 consisted in a linear gradient of acetonitrile (A) and an aqueous solution of formic acid
166 (0.1% w/w) (B); the composition of the eluent changed from 5% of A to 50% of A in
167 8.5 min and the flow rate was 0.3 mL min^{-1}. Detection wavelength was 230 nm. The
168 identification and quantification of the pollutants were carried out by comparison with
169 standards. Samples were filtered through polypropylene filters (VWR, 0.45 μm) before
170 analysis.

171 The fluorescence EEM of the samples were recorded using a modular fluorimeter
172 QuantaMaster (PTI) by a subsequent emission scanning from 300 to 600 nm at 5 nm
173 increments by varying the excitation wavelength from 250 to 550 nm at 5 nm
174 increments.

175

176 2.4. Statistic analysis

177 The effect of three operational parameters (pH, ozone doses and pollutants
178 concentration) on the ozonation and combination ozone/UVA-Vis process was studied
179 using an experimental design methodology. As phenolic concentration varies depending
180 the effluent, the range 8-48 mg/L was chosen to be high enough to obtain reliable
181 kinetics by HPLC analysis and not as high to saturate the response of EEM or toxicity
182 experiment concentrations; ozone dosage was also tuned in a low domain to avoid too
183 fast reactions and to allow and accurate sampling . For this purpose, a Doehlert matrix
184 was used in order to select the experimental points required to obtain a three-
185 dimensional response surface; this methodology was chosen because it minimizes the
186 number of experiments required to obtain the n-dimensional surface response (Ferreira
187 et al., 2004). To this end, a total of 15 experiment were chosen: 13 combinations of the
188 three variables studied and two replicates of the central point (see Table 1 for detailed
189 experimental conditions). The software Statgraphics Centurion XVI was used for
190 response surface model fitting by means of the least squares method. The treatment time
191 required to decrease in an 80% the sum of the concentration of the 6 pollutants that
192 could be analysed via liquid chormatography ($t_{80\%}$), was used as response. This type of
193 parameters have been used in previous papers for statistical analysis as it provides a
194 more "visual" information of the time required to achieve the desired result when
195 compared with with pseudo-first order kinetic constants (Gomis et al., 2015, García-
196 Ballesteros et al., 2017; Caram et al., 2018). In particular $t_{80\%}$ was chosen in order to
197 ensure that a significant degradation of the pollutants occurred (80%) and to avoid the
198 asymptotic behaviour of the concentration vs time plot observed at values close to 100%
199 degradation and that results in important errors in the determination of the required time
200 of treatment.

2.5 Bioassays

Bioassays employed in this work have been described in detail elsewhere (García-Ballesteros et al., 2016). Toxicity tests based on *P. subcapitata* were performed according to ISO 8692:2012. Briefly, microplates were filled with the test dilutions and controls, and inoculated with 10^4 cells/mL being the he total volume of each well 300 µL. Microplates were incubated at 23 ºC under continuous illumination (6000-10000 lux), saturated with 2% CO_2 and stirred at 120 rpm. The algal growth was measured by *in-vivo* chlorophyll fluorescence every 24 h, (until 72 h) using a microplate reader (Tecan Infinite M200).

Assays based on the inhibition of the mobility of *D. magna* (ISO 6341:2012) used 24-h old daphnids hatched from the ephippia. Five individuals were placed in 15 mL recipients containing 10 mL of test dilution and corresponding controls. The assays were conducted in the dark at a constant temperature of 21 ºC.

For the RYA (Recombinant Yeast Assay), yeast cells were grown overnight in a synthetic medium. Assays were performed in a polypropylene microplate (NUNC™, Roskilde, Denmark). After plates incubation (6 h at 30 °C at 120 rpm in orbital shaker), were added sequentially Y-PER (30 °C, 30 min) and then, enzymatic substrate. After centrifugation, β-galactosidase activity was monitored using a spectrofluorometer (TECAN Infinite M2000). The relative activity of β-galactosidase was calculated from recorded activity of positive and negative control. Results were calculated as E2 equivalents (EEQ) (estrogenic activity) or β-NF (BNFEQ) (dioxin-like activity), defined as the concentration (ng/L) of standard that should be present to account for the observed response.

3. Results and discussion

3.1. Ozonation of the phenolic compounds

The mixture of all eight phenols and polyphenols was treated by means of O_3 under the following experimental conditions (initial concentration of each pollutant = 3.5 mg/L; O_3 dose = 0.2 g/h and pH = 7.5). Only six of them could be analysed by liquid chromatography (tannic and ellagic acids were not detected, most probably due to their high molecular weight). Plots of the relative concentration of all six pollutants (C/Co, where C is the concentration at the sampling time and Co the initial concentration of each pollutant) vs time were obtained (Figure 1a). In general, very fast elimination of the studied pollutants was observed (complete removal in a few minutes in all cases), being the 2,4-dinitrophenol the more reluctant to the treatment (ca. 20 min of ozonation).

In order to gain further insight into the effect of ozone on the mixture of phenols and polyphenols, a set of experiments was carried out in order to determine the effect of pH, ozone dose and initial pollutants concentration. Based on these data, the $t_{80\%}$ was calculated in each experiment by interpolation from the time profile of the relative concentration of the six detected pollutants (Table 1). A three-dimensional full quadratic response surface model was obtained (Eq 1), where O_3-D is the ozone dose given in g/h and [P] is the pollutants concentration (mg/L); $t_{80\%}$ is expressed in minutes:

$$t_{80\%} = 12.36 - 13.31 \cdot O_3\text{-}D - 1.86 \cdot pH + 0.83 \cdot [P] + 4.32 \cdot O_3\text{-}D^2 + 1.05 \cdot O_3\text{-}D \cdot pH - 0.55 \cdot O_3\text{-}D \cdot [P] + 0.07 \cdot pH^2 - 0.03 \cdot pH \cdot [P] - 0.015 \cdot [P]^2 \quad \text{(Equation 1)}$$

252

253 The value of the determination coefficient was high ($R^2 = 0.92$), indicating good
254 correspondences between experimental data and calculated values of $t_{80\%}$. Pareto charts,
255 (Figure 2a), indicate that, only pH, its quadratic term (pH^2), interaction of pH with O_3
256 and O_3 were significant; Taking this into account, equations can be reformulated as
257 follows:

258 $t_{80\%} = 12.36 - 13.31 \cdot O_3\text{-}D - 1.86 \cdot pH + 1.05 \cdot O_3\text{-}D \cdot pH + 0.07 \cdot pH^2$ (Equation 2)

259

260 In order to better analyse the results, two-dimensional contour plots can be obtained
261 from the three-dimensional curve given by the model by fixing one of the variables at
262 the desired value (Figure 3). First, pH was fixed at an acidic (pH = 5) and a basic value
263 (pH = 10). At low pH, time required to remove the pollutants decreases with increasing
264 ozone dosages; on the other hand at basic pH the reaction is always faster and the effect
265 of ozone dosage is not so evident. This result might be due to the different mechanisms
266 operating at both media: while the attack of molecular ozone is predominating at low
267 pH, decomposition of this reagent into more reactive hydroxyl radicals occurs at pH =
268 10; furthermore, ozone decomposition at basic pH also favours its transfer into the
269 liquid phase increasing the utilization rate of ozone. For this reasons, when operating
270 the most efficient mechanism, less ozone is needed. When looking at the surface
271 obtained at pH = 10, two regions can be identified where reaction rate is lower: a) at
272 low ozone amount and high concentration of pollutants, most probably due to the lack
273 of oxidizing agent, and b) at high ozone amounts, when recombination of radicals might
274 decrease the efficiency of ozonation (Chavez, 2016), or because hydroxyl radical

participates in the chain decomposition cycle of ozone when this reagent is found at high concentrations.

Another plot was obtained by fixing the concentration of pollutants at the central point (3.5 mg/L) in order to check the effect of pH and ozone dosage (Figure 4). Similar trends were also observed: a) best results were observed at basic pH because of the prevalence of radical-mediated mechanism; b) an strong interaction between ozone dosage and pH was observed (increasing pH required lower ozone dosages to reach the same % of degradation) and c) a slight decrease in efficiency was observed at highest ozone amounts at basic media.

Finally, ozone dosage was fixed at a low (0.3 g/h) and a high value (0.8 g/h). The effect of pH was predominating, being the reaction faster at basic media. However, some differences could be observed: a) at low ozone dosage, a pH increase resulted in an acceleration of the process in all the studied domain, and pollutant concentration had a slight influence on the process (higher pH was required to reach the same reaction rate at increasing pollutant concentration) and b) on the contrary, at high ozone dosage, the effect of pollutant concentration is not significant and pH also plays a lower role, decreasing the efficiency at high pHs, again in this case because of the detrimental effect of hydroxyl radicals, via recombination or alteration of the ozone cycle.

As a consequence, of these data, the following conclusions can be obtained: a) at acidic pH and low ozone dosage, the reaction is inefficient, b) increasing both parameters, represents an enhancement in the process, and c) interaction of basic pH and high

amounts of ozone decreases the efficiency of the process. Finally, it is worthy to indicate that being the amount of ozone between 0.2 and 1 g/h and the $t_{80\%}$ between 1 and 2 min in most cases, the amount of ozone supplied to the reactor can be estimated in 3-30 mg; in the central point, 10 mg where needed, that accounted for ca. 40 mg/L. However, this value should not be overemphasised as may strongly depend in the characteristics of the reactor.

3.2. Combination of ozonation and UV-vis irradiation

The combination of O_3 and UV-VIS was also studied; although the overlap between the light emitted by the xenon lamp (and that was not cut off by the Pyrex filter, namely $\lambda >$ 300 nm) and the absorption of ozone in water is very low, in some cases slight increases in the efficiency of the process might be of interest (always excluding highly coloured effluents). Time resolved profiles of C/Co were obtained (see Figure 1b for an example). Again in this case, Doehlert matrixes were used, based in the same experimental points used in the O_3 experiment, being $t_{80\%}$ the response parameter (see Table 1): An equation was obtained (eq. 3) with a regression coefficient of 0.99.

$$t_{80\%} = 3.22 - 0.78 \cdot O_3\text{-}D - 0.46 \cdot pH + 0.38 \cdot [P] - 0.96 \cdot O_3\text{-}D^2 - 0.06 \cdot O_3\text{-}D \cdot pH - 0.03 \cdot O_3\text{-}D \cdot [P] + 0.03 \cdot pH^2 - 0.06 \cdot pH \cdot [P] - 0.0 \cdot [P]^2 \quad \text{(eq. 3)}$$

320 Pareto charts showed that the same parameters as in O_3 were found, except that for
321 O_3/UVA-vis also pollutant concentration became significant (Figure 2b). Hence,
322 equation 3 can be reformulated as equation 4

323

324 $t_{80\%} = 3.22 - 0.78 \cdot O_3\text{-D} - 0.46 \cdot pH + 0.38 \cdot [P] - 0.06 * O_3\text{-D} * pH + 0.03 \cdot pH^2$ (eq. 4)

325

326 Figure 4 shows the bi-dimensional contour plots obtained by fixing all three variables in
327 a mid-value. When [P] = 3,5 mg/L, the pH was the predominating factor, although at
328 basic media increasing O_3 dose resulted in a process enhancement. When pH value was
329 fixed, highest efficiency was observed at high O_3 dose and low [P]. Finally, for O_3 dose
330 = 0.6 g/h, highest reaction rates were observed at basic pH and high pollutants
331 concentration.

332

333 However, it seems more interesting to see the synergic effect of O_3 and simulated
334 sunlight. Too clarify this point, the subtraction of $t_{80\%}$ obtained by O_3 minus $t_{80\%}$
335 obtained with O_3/UVA-Vis was calculated (Figure 5). Negative values indicate that
336 UVA-vis is able to enhance the process. In general this happens at low pH values and
337 low ozone dosages, indicating that this combination is meaningful in those regions
338 where ozonation is inefficient.

339

340 3.3. Fluorescence measurements

341

As two of the compounds could not be detected, and analysis and identification of intermediates is difficult in such a complex mixture, using alternative analytical seems interesting. An attractive possibility is employing the fluorescence emission-excitation matrixes. They consist of bi-dimensional plots of the emission of a sample at a given wavelength (λ_{em}) when excited at another wavelength (λ_{exc}). According to the regions of the matrix where signals can be found, some information on the nature of the organics present in the samples can be obtained (García-Ballesteros et al., 2017). Excitation emission matrices (EEMs) were recorded for both processes (O_3 and O_3/ UVA-VIS combination, Figure 6 and 7 respectively) in the central point conditions at different treatments time. The EEM for each individual pollutant can be found elsewhere (García-Ballesteros et al., 2016). A constant decrease in the fluorescence emission can be observed in the area where $\lambda_{ex} < 300$ nm and $\lambda_{em} < 400$ nm. In sharp contrast, there was a significant increase in the signal in the region 300 nm $< \lambda_{ex} <$ 350 nm and 420 nm $< \lambda_{em} <$ 470 nm, to reach a maximum value in the sample taken after 1 or 2 min of reaction. Then, there was also some decrease in this signal, which became very weak beyond 8 min of irradiation. These trends were clearer in the O_3/irradiation combination. This behaviour is an indicator of the generation of intermediates along the process, which are responsible for the signal with maximum at ca. $\lambda_{ex} = 325$ nm and $\lambda_{em} = 450$ nm; they might be associated to quinones/hydroquinones, which are expected to be intermediates in the oxidation of aromatic rings and whose signal is compatible with that of the EEM (Cory et al., 2005).

In order to gain further insight into the information provided by the EEM, PARAFAC was applied to a set of experiments consisting in all the matrixes obtained in the O_3 and O_3/UV-vis. This mathematical procedure is able to decompose the EEM into more

simple components. Models with 3-8 components were tested and results were more consistent with that considering 4 components (C1-C4); info. The evolution of the score of each component vs. time can be found in supporting Figure 8 a and b for O_3 and O_3/UV-vis combination, showing in both cases similar trends. For the samples recorded at t = 0 min, the highest score was reached by C4 and beyond this point, a continuous decrease of this component can be observed; hence, C4 might be associated with the parent phenolic compounds, that are degraded in the early stages of the process (5-8 min). On the other hand, C2 and C3 suffer an initial increase in the score, followed by a decrease, which is compatible with associating these components with intermediates formed in the oxidative process. Finally, C1 follows a continuous increase throughout the process, and might represent more oxidized by-products.

3.3. Bioassays

As complete mineralization of the sample could not be achieved and formation of reaction by-products is evident according to the results shown in the previous sections, monitoring changes in the toxicity of the mixture along the treatment seems meaningful. As done with the photo-Fenton process (García-Ballesteros at al., 2016) different bioassays were performed in order to monitor changes in toxicity. The chosen experimental conditions were: a initial concentration of 6 mg/L of each pollutant, pH = 9 and ozone dosage of 0.8 g/h (corresponding to point 4 in the experimental plot). They were chosen in order to ensure relatively fast reaction and, at the same time, to have an important concentration of intermediates in the solution. In fact, all the phenolic compounds were removed after 10 min of treatment, but 70 % of the DOC still

391 remained after 30 min of treatment. Results are shown in Table 2. The initial sample
392 was highly toxic, as according to both, *D. magna* and *P. subcapitata* experiments, 100
393 % toxicity was measured; in the initial stages of the process, a fast detoxification was
394 recorded and beyond 5 min of treatment measured values were systematically below
395 30%, what indicated that samples were scarcely toxic. A similar behaviour was
396 observed for the estrogenic and dioxin-like properties, as the initial sample gave values
397 equivalent to more than 11000 ng/L of dioxine and 75 ng/L of E2 (for sample at t = 1
398 min, as the untreated sample was too toxic to measure estrogenic activity). Ozonation
399 resulted in a fast decrease in both parameters and the estrogenic activity was completely
400 removed after 30 min of ozonation and the dioxin-like behaviour decreased three order
401 of magnitude.

402

403 **4. Conclusions**

404 In this paper a methodology combining experimental design methodology, liquid
405 chromatography, excitation emission matrixes (EEM) and bioassays has been tested and
406 a satisfactory assessment of the decontamination process has been achieved, even when
407 pollutants that cannot be analysed by HPLC are present in the initial sample.
408 Complementary information has been obtained according to the different analytical
409 methods: HPLC analyses have been employed to monitor the removal of the parent
410 phenolic pollutants and, based on these data, experimental design methodology is useful
411 to determine favourable experimental conditions for ozonation, as well as to evaluate
412 the convenience of combining O_3 and UVA-vis irradiation.

413

414 The scarce mineralization reached indicate formation of reaction by-products. EEM
415 combined with PARAFAC analysis is a good technique to gain further insight into the
416 nature of these intermediates, as well as for those pollutants that cannot be detected by
417 HPLC analyses. Finally, a battery of bioassays allows having a reliable monitoring of
418 the toxicity of the samples along the chemical oxidative processes.

419

420 **Acknowledgements**

421 The authors want to thank the financial support of the European Union (PIRSES-GA-
422 2010-269128, EnvironBOS) and Spanish Ministerio de Educación y Ciencia
423 (CTQ2015-69832-C4-4-R). Sara García-Ballesteros would like to thank Spanish
424 Ministerio de Economía y Competitividad for her fellowship (BES-2013-066201)

425

426 **References**

427 Amat, A.M., Arques, A., Beneyto, H., García, A., Miranda, M.A. Seguí, S., 2003.
428 Ozonisation coupled with biological degradation for treatment of phenolic pollutants: a
429 mechanistically based study. Chemosphere 53, 79–86.

430 Beltrán, F.J., 2003. Ozone Reaction Kinetics for Water and Wastewater Systems (Boca
431 Raton, FL: Lewis Publishers).

432 Caram, B., García-Ballesteros, S., Santos Juanes, L., Arques, A., García Einschlag, F.S.,
433 2018. Humic-like substances for the treatment of scarcely soluble pollutants by mild
434 photo-Fenton process. Chemosphere, 198, 139-146.

435 Chávez, A.M., Rey, A., Beltrán F.J., Álvarez P.M., 2016. Solar photo-ozonation: A
436 novel treatment method for the degradation of water pollutants. J. of Hazardous
437 Materials 317, 36–43.

438 Chen, W., Westerhoff, P., Leenheer, J.A., Booksh, K. 2003. Fluorescence
439 excitation−emission matrix regional integration to quantify spectra for dissolved organic
440 matter. Environ. Sci. Technol. 37, 5701–5710.

441 Collivignarelli C1., Sorlini S., 2004. AOPs with ozone and UV radiation in drinking
442 water: contaminants removal and effects on disinfection byproducts formation. Water
443 Sci Technol. 49(4), 51-6.

444 Cory, R.M., Mcknight, D.M., 2005. Fluorescence spectroscopy reveals ubiquitous
445 presence of oxidized and reduced quinones in dissolved organic matter. Environ.Sci.
446 Technol. 39, 8142-8149.

447 Dodd, M. C., Kohler, H. E., Von Gunten, U., 2009. Oxidation of antibiotic compounds
448 by ozone and hydroxyl radical: elimination of biological activity during aqueous
449 ozonation processes. Environ. Sci. Technol., 43, 2498.

450 Ferreira, S.L.C., dos Santos, W. N. L., Quintella, C.M., Neto, B. B., Bosque-Sendra,
451 J.M., 2004. Doehlert matrix: a chemometric tool for analytical chemistry – review.
452 Talanta 63, 1061-1067.

453 García-Ballesteros, S., Mora, M., Vicente, R., Sabater, C., Castillo, M.A., Arques A.,
454 Amat, A.M., 2016. Gaining further insight into photo-Fenton treatment of phenolic
455 compounds commonly found in food processing industry. Chem Eng. J. 288, 126-136.

456 García Ballesteros, S., Constante, M., Vicente, R., Mora, M., Amat, A.M., Arques, A.,
457 Carlos, L., García Einschlag, F. S., 2017. Humic-like substances from urban waste as

458 auxiliaries for photo-Fenton treatment: a fluorescence EEM-PARAFAC study.
459 Photochem. Photobiol. Sci., 16, 38-45.

460 Garoma, T., Gurol, M.D., 2005. Modeling Aqueous Ozone/UV Process Using Oxalic
461 Acid as Probe Chemical. Environ. Sci. Technol. 39, 7964-7969.

462 Gomis, J., Carlos, L., Bianco Prevot, A., Teixeira, A. C. S. C., Mora, M., Amat, A.M.,
463 Vicente, R., Arques, A., 2015. Bio-based substances from urban waste as auxiliaries for
464 solar photo-Fenton treatment under mild conditions: optimization of operational
465 variables. Catal. Today, 240, 39-45.

466 Ikehata, K. and El Din, M.G. , 2004. Degradation of recalcitrant surfactants in
467 wastewater by ozonation and advanced oxidation process. A review. Ozone Sci. Eng.
468 26, 327-343.

469 Ikehata, K., Naghashkar, N.J. and El Din, M.G. , 2006. Degradation of aqueous
470 pharmaceuticals by ozonation and advanced oxidation process. A review. Ozone Sci.
471 Eng. 28, 3537-414.

472 Kuo, W.S., 1999. Synergistic effects of combination of photolysys and ozonation on
473 destruction of chlorophenols in water. Chemosphere, 39, 1853-1860.

474 Legrini, O., Oliveros, E., and Braun, A.M., 1993. Photochemical Processes for Water-
475 Treatment, Chem. Rev., 93(2):671–698.

476 Liu, C., Tang, X., Kim, J., Korshin, V., 2015. Formation of aldehydes and carboxylic
477 acids in ozonated surface water and wastewater: A clear relationship with fluorescence
478 changes. Chemosphere 125, 182–190.

479 Liu, C., Li, P., Tang, X., Korshin, V., 2016. Ozonation effects on emerging
480 micropollutants and effluent organic matter in wastewater: characterization using

481 changes of three-dimensional HP-SEC and EEM fluorescence data. Environ Sci Pollut
482 Res. 23:20567–20579.

483 Lovato, M.E., Fiasconaro, M. L., Martín, C. A., 2017. Degradation and toxicity
484 depletion of RB19 anthraquinone dye in water by ozone-based technologies. Water
485 Science and Technology, 75(4), 813-822.

486 Luis, P., Saquib, M.,Vinckier, C., Van Der Bruggen, B., 2011. Effect of membrane
487 filtrationon ozonation efficiency for removal of atrazine from surface water. Ind.
488 Eng.Chem.Res. 50, 8686-8692.

489 Mangalgiri, K.P., Timko, S.A., Gonsior, M. Blaney, L., 2017. PARAFAC Modeling of
490 Irradiation- and Oxidation-Induced Changes in Fluorescent Dissolved Organic Matter
491 Extracted from Poultry Litter. Environ. Sci. Technol., 51 (14, 8036–8047.

492 Márquez, G., Rodriguez, E.M., Beltrán, F.J., Álvarez P.M., 2014. Solar photocatalytic
493 ozonation of a mixture of pharmaceutical compounds in water. Chemosphere 113, 71–
494 78.

495 Mendoça, E., Pereira, P., Martins, A., Anselmo, A.M., 2004. Fungal and Detoxification
496 of Cork Boiling Wastewaters. Engin Life Sci. 4 (2), 144-149.

497 Mizuno, T., Ohara, S., Nishimura, F., Tsuno, H., 2011. O_3/H_2O_2 process for both
498 removal algal-derivated compounds and controlo f bromate ion formation. Ozone Sci.
499 and Eng., 33, 121-135.

500 Oh, J.S., Yajima, H., Hashida, K., Ono, T., Ishijima, T., Serizawa, I., Furuta, H., Hatta,
501 A., 2016. In-situ UV Absorption spectroscopy for observing dissolved ozone in water. J.
502 Photopolymer Sci. Technol., 29, 427-432.

503 Orge, C.A., Pereira, M.F.R., Faria J.L., 2017. Photocatalytic-assisted ozone degradation
504 of metolachlor aqueous solution. Chem. Eng. J., 318, 247-253.

505 http://peschl-
506 ultraviolet.com/cms/upload/bilder_produktseiten/1_photochemie/1_praeparative_photoc
507 hemie/mpds-basic/bilderset/spektren/txe150_en.jpg

508 Quiñones, D.H., Álvarez, P.M., Rey, A., Contreras, S., Beltrán. F.J., 2015. Application
509 of solar photocatalytic ozonation for the degradation of emerging contaminants in water
510 in a pilot plant. Chemical Engineering Journal 260, 399–410.

511 Ribeiro, A.R., Nunes, O.C., Pereira, M.F.R., Silva, A.M.T., 2015. An overview on the
512 advanced oxidation process applied for the treatment of water pollutants defined in the
513 recently launched Directive 2013/39/EU. Environmental International, 75, 33-51.

514 Rivas, L., Beltran F.J., Encinas, 2012. A. Removal of emergent contaminants:
515 Integration of ozone and photocatalysis. J. of Env. Management, 100, 10-15.

516 Siqueira F., Amaral, L., 2015. Degradation of caffeine by advanced oxidative processes:
517 O_3 and O_3/UV. Ozone Sci. & Eng., 37, 379-384.

518 Tichonovas, M., Krugly, E., Jankunaite, D., Racys, V., Martuzevicius, D., 2017. Ozone-
519 UV-catalysis based advanced oxidation process for wastewater treatment.
520 Environmental Sci. Pollut. Res., 224, 17584-17597.

521 Vilar, V.J.P., Maldonado, M.I., Oller, I., Malato, S., Boaventura, R.A.R., 2009. Solar
522 treatment of cork boiling and bleaching watewaters in a pilot plant. Water Research. 43
523 (16), 4050-4062.

524 Zhang, J., Wu, Y., Qin, C., Liu, L., Lan, Y., 2015. Rapid degradation of aniline in
525 aqueous solution by ozone in the presence of zero-valent zinc. Chemosphere, 141, 258-
526 264.

527

528

529

530 Table 1: Experimental points and response (t_{80}) used in the experimental design

531 methodology based on Doehlert matrix)

Experiment number	[O_3] (g/h)	pH	[Pollutant] (mg/L)	$t_{80\%}$ O_3 (min)	$t_{80\%}$ O_3/UVA-VIS (min)
1	0.6	7.5	3.5	1.54	1.65
2	1	7.5	3.5	1.29	0.91
3	0.8	12	3.5	0.95	1.03
4	0.8	9	6	1	1.06
5	0.2	7.5	3.5	2.34	1.73
6	0.4	3	3.5	6.26	3.10
7	0.4	6	1	1.53	1.72
8	0.8	3	3.5	2.44	2.97
9	0.8	6	1	0.99	1.38
10	0.4	12	3.5	0.97	1.37
11	0.6	10.5	1	0.85	1.57
12	0.4	9	6	1.38	1.53
13	0.6	4.5	6	2.93	3.15
14	0.6	7.5	3.5	0.93	1.42
15	0.6	7.5	3.5	0.9	1.35

532

533

534 Table 2: Toxicities measured by a battery of bioassays for samples taken after different
535 ozonation periods (initial concentration of 6 mg/L, pH = 9 and ozone dosage of 0.8 g/h).

536

t (min)	**Toxicity (%)**		**Estrogenic activity**	**dioxin-like behaviour**
	D. magna	*P. subcapitata*	**E2 (ng/L)**	**(ng/L)**
0	100	100	Very toxic	11342
1	5	30	75.7	14464
2	50	20	11.4	22.5
5	30	25	45.3	82.4
10	20	26	7.3	166.2
30	25	3	--	107.5

537

538

539

540

541

542

543

544

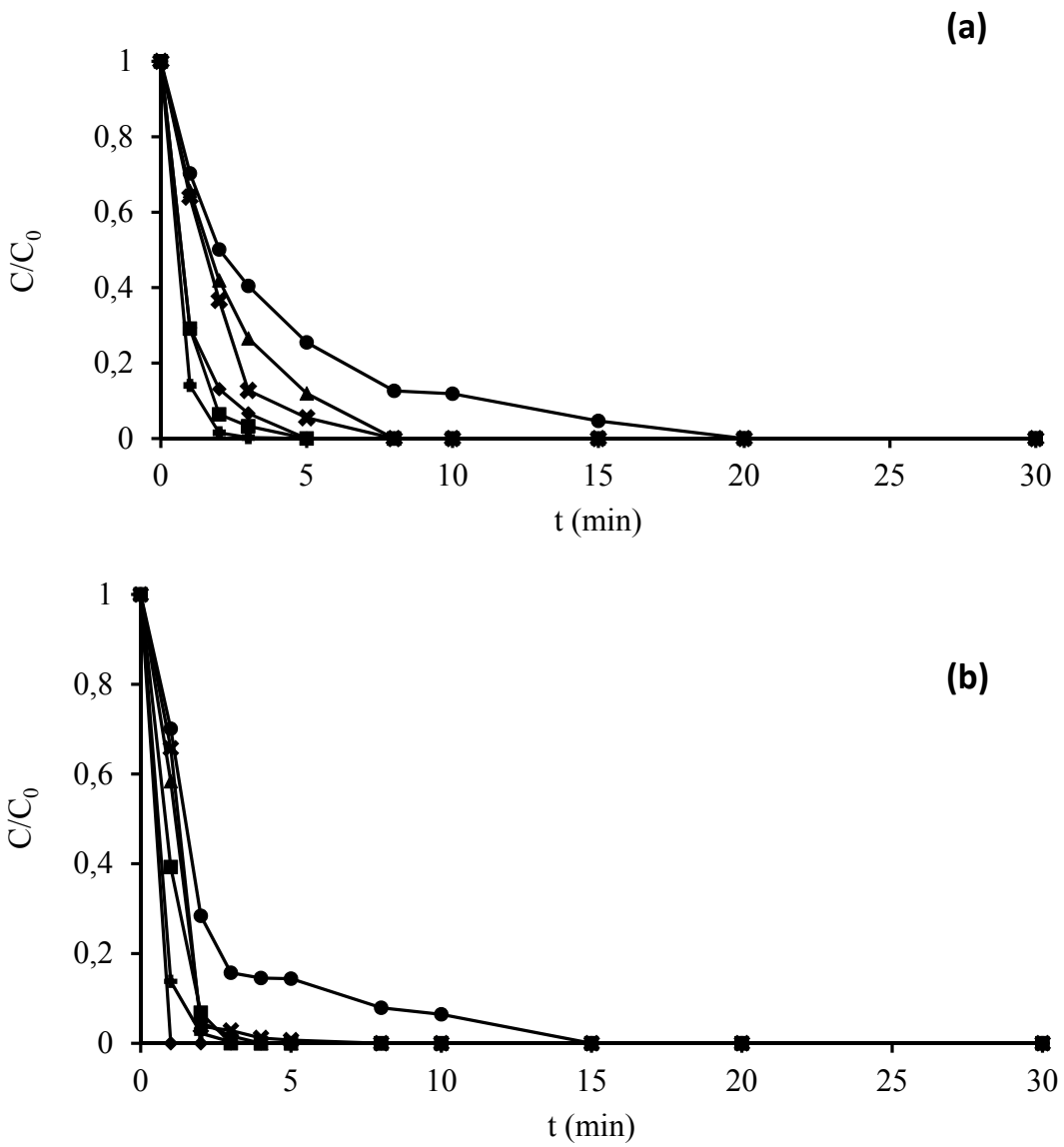

Figure 1: Ozonisation (a) and O_3/UVA-VIS combination (b) for the removal of a mixture of phenolic compounds: initial concentration of each pollutant = 3.5 mg/L; O_3 dose = 0.2 g/h and pH = 7.5. A plot of the relative concentration of each pollutant vs. time is given: gallic acid (♦); protocatechuic acid (■); vanillic acid (▲); sinapic acid (+); syringic acid (×) and 2,4-dinitrophenol (●).

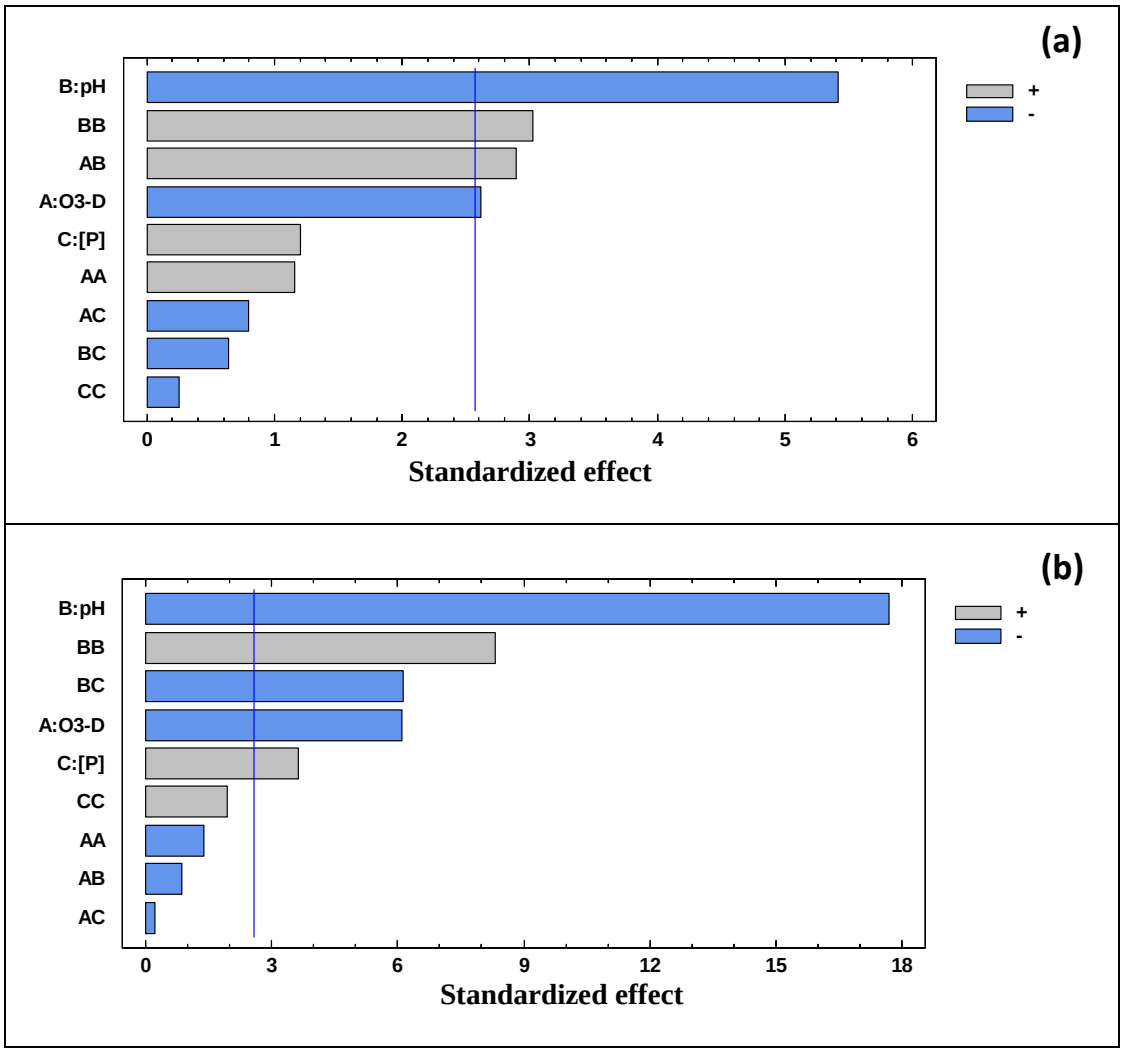

552

553 Figure 2: Pareto charts for the response $t_{80\%}$ (min) obtained for the ozonisation (a) and

554 the O_3/UVA-VIS combination (b) for the degradation of a mixture of six phenolic

555 compounds.

556

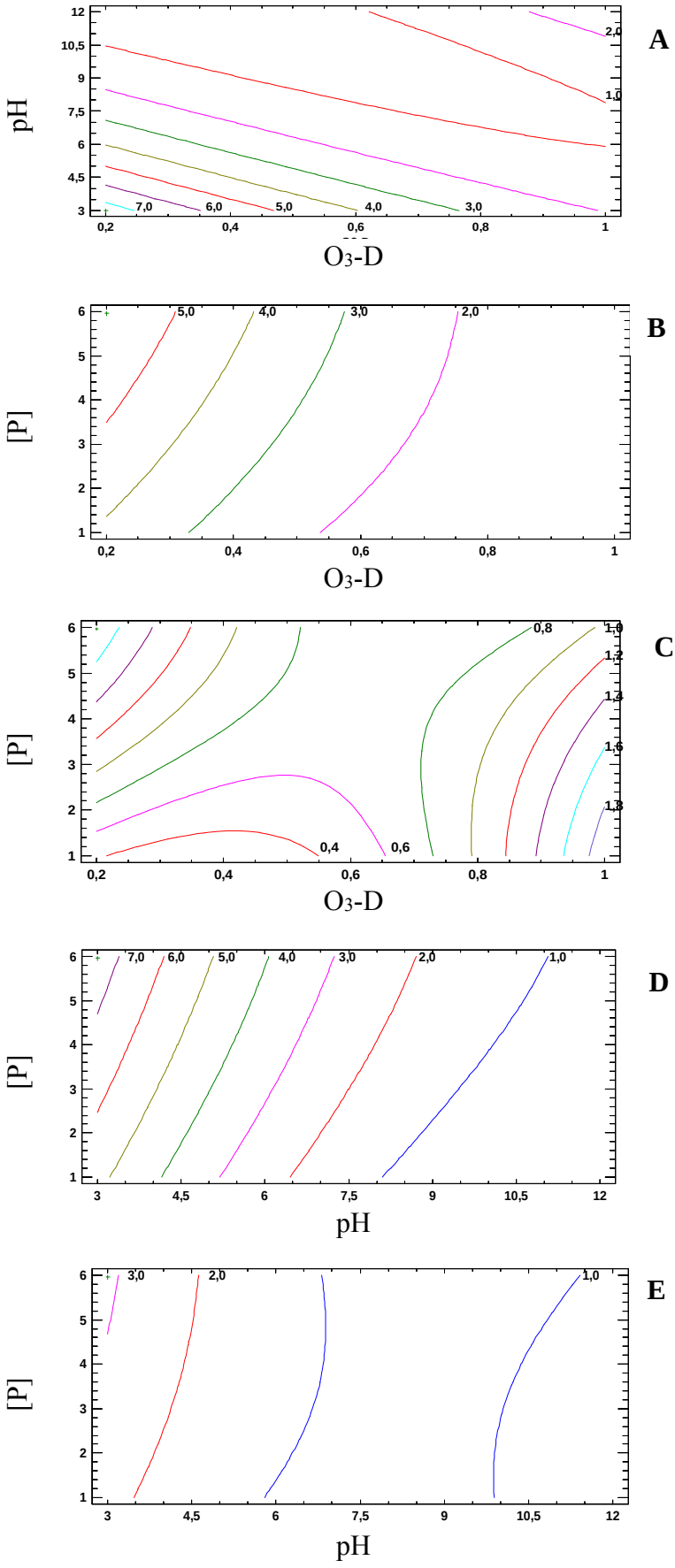
A
pH
O3-D
7,0
6,0
5,0
4,0
3,0
2,0
1,0
B
[P]
O3-D
C
[P]
O3-D
0,4
0,6
0,8
D
[P]
pH
E
[P]
pH

557

558 Figure 3: Two-dimensional contour plots for $t_{80\%}$ (min) obtained for the removal of a
559 mixture of six phenolic compounds by ozonisation by fixing one parameter at a desired
560 value. A) [P] = 3.5 mg/L, B) pH = 5, C) pH = 10, D) O_3-D = 0.3 g/h, E) O_3-D = 0.8 g/h.

561

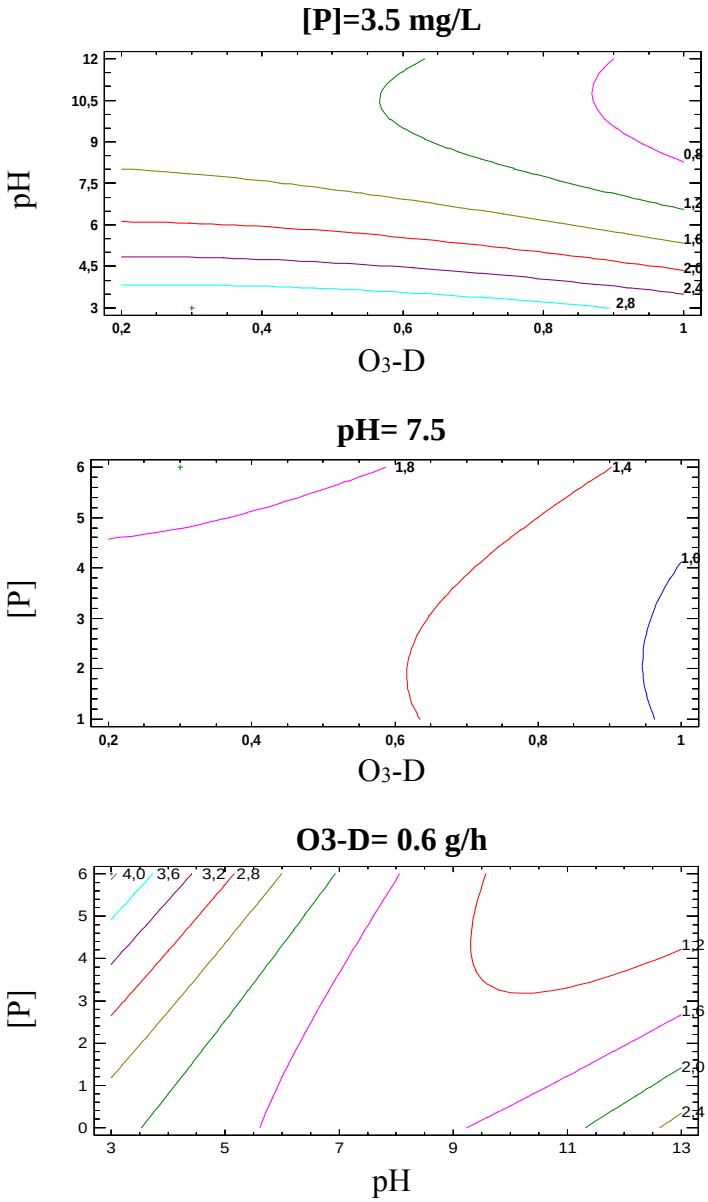

Figure 4. Contour plots obtained for the removal of a mixture of six phenolic compounds by O_3/UVA-Vis combination. Value of $t_{80\%}$ (min) at fixed values in the midpoint of the three different factors (O_3-D, pH and [P] employed in the Dohelert design.

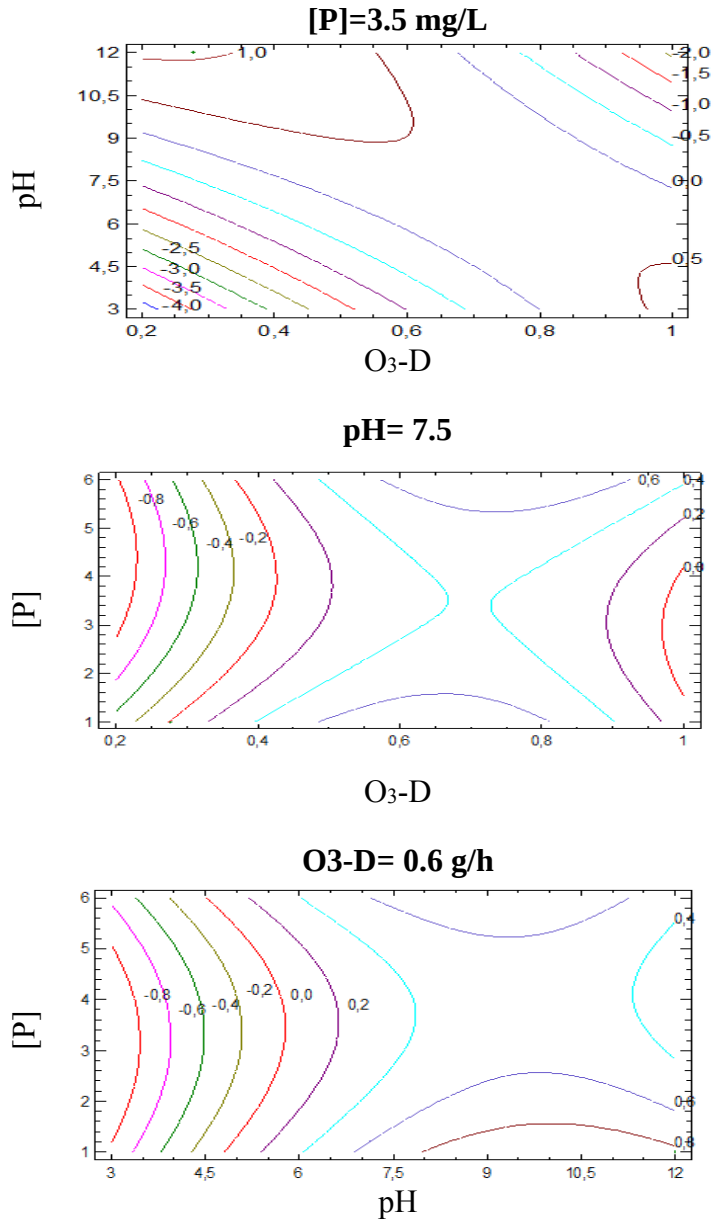

570

571 Figure 5. Contour plots obtained for the difference of $t_{80\%}$ in the combination O_3/UVA-

572 Vis and O_3. Negative values show that UVA-vis is able to enhance the process.

573

574

575

576

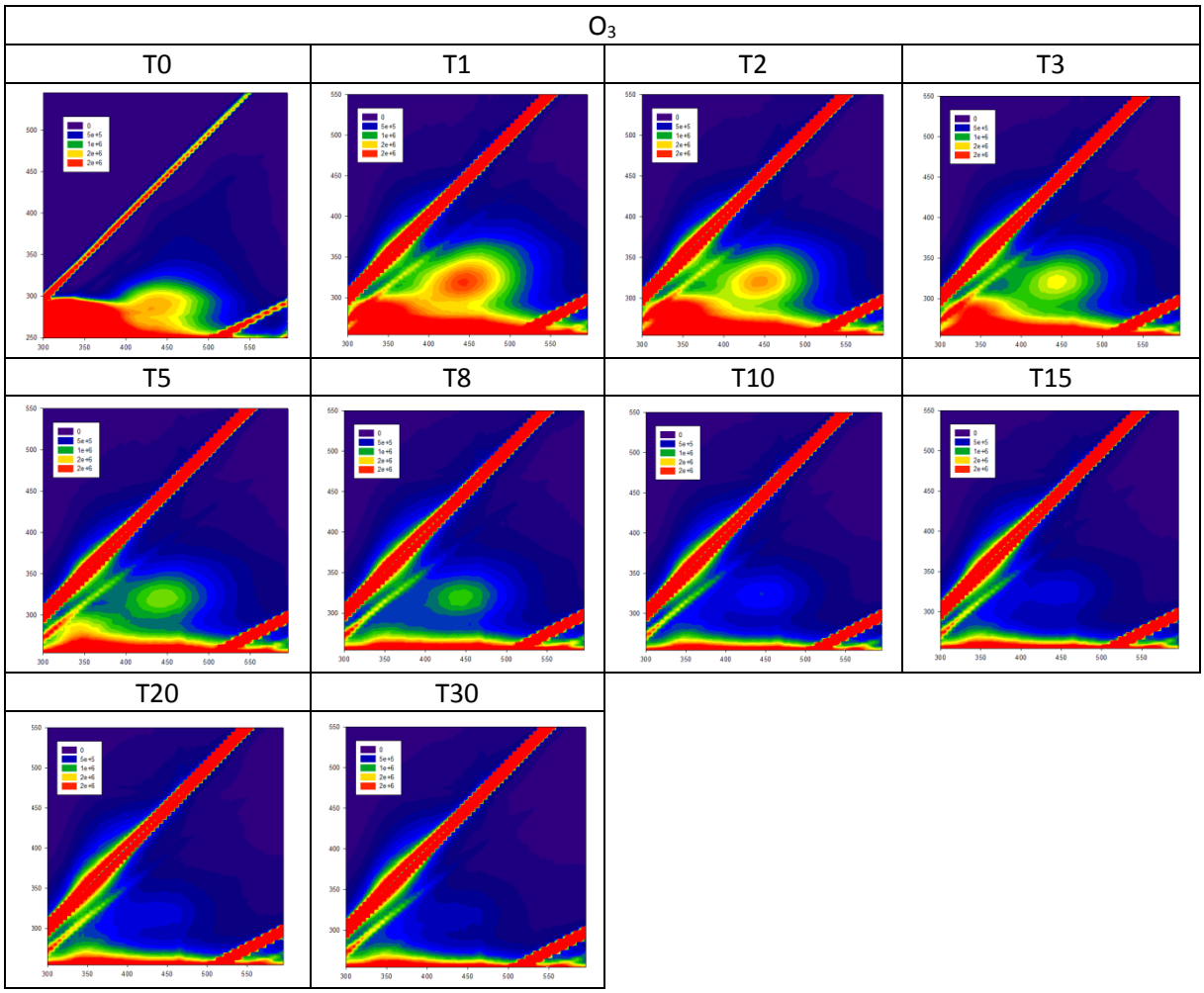

Figure 6: EEMs obtained for the removal of a mixture of six phenolic compounds by O_3 at different treatments times. Figures shows the excitation area (Y-axis) between 250 and 550 nm, the emission area (X-axis) between 300 and 600 nm and the fluorescence intensity in the 0 and 2 x 10^6 range.

590

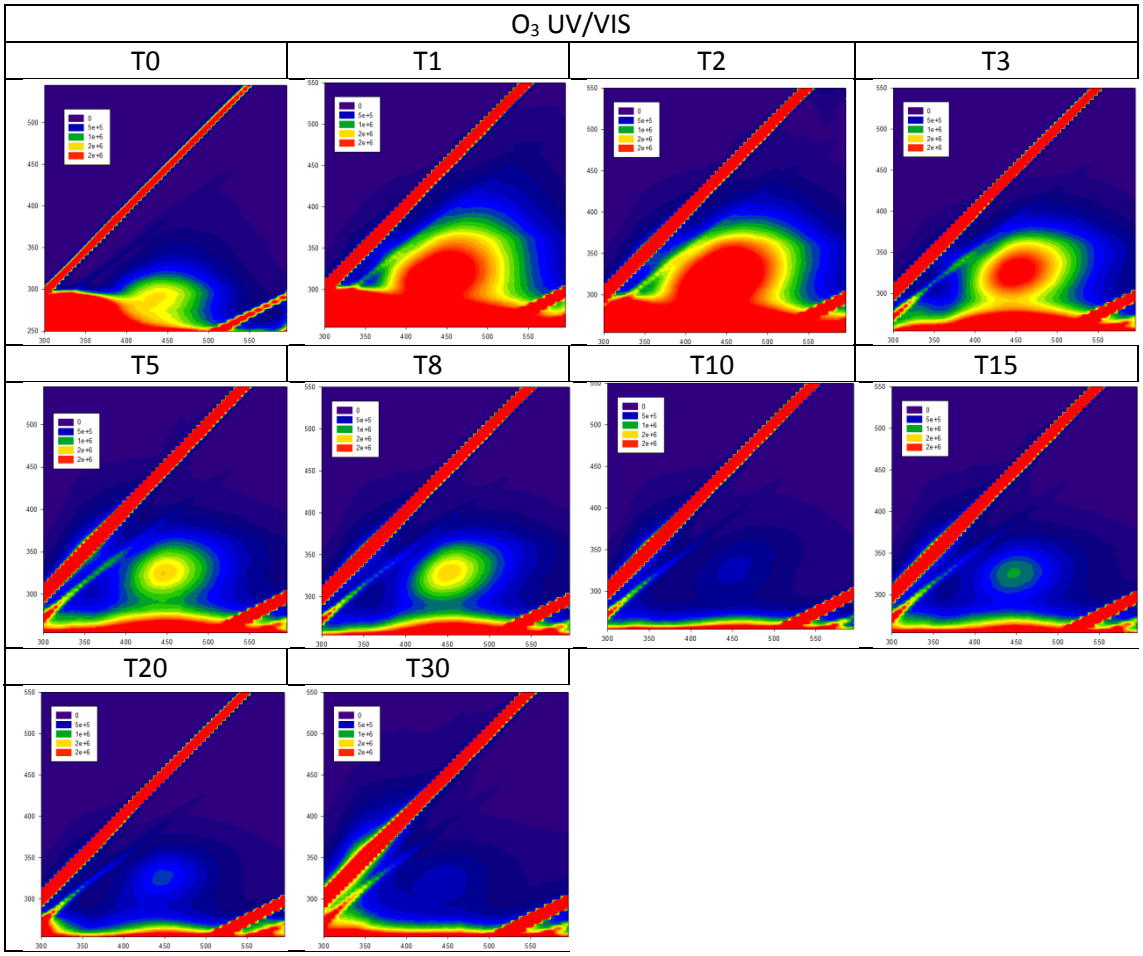

591

592

593 Figure 7: EEMs obtained for the removal of a mixture of six phenolic compounds by

594 O_3/UVA-VIS combination at different treatments times. Figures shows the excitation

595 area (Y-axis) between 250 and 550 nm, the emission area (X-axis) between 300 and 600

596 nm and the fluorescence intensity in the 0 and 2 x 10^6 range.

597

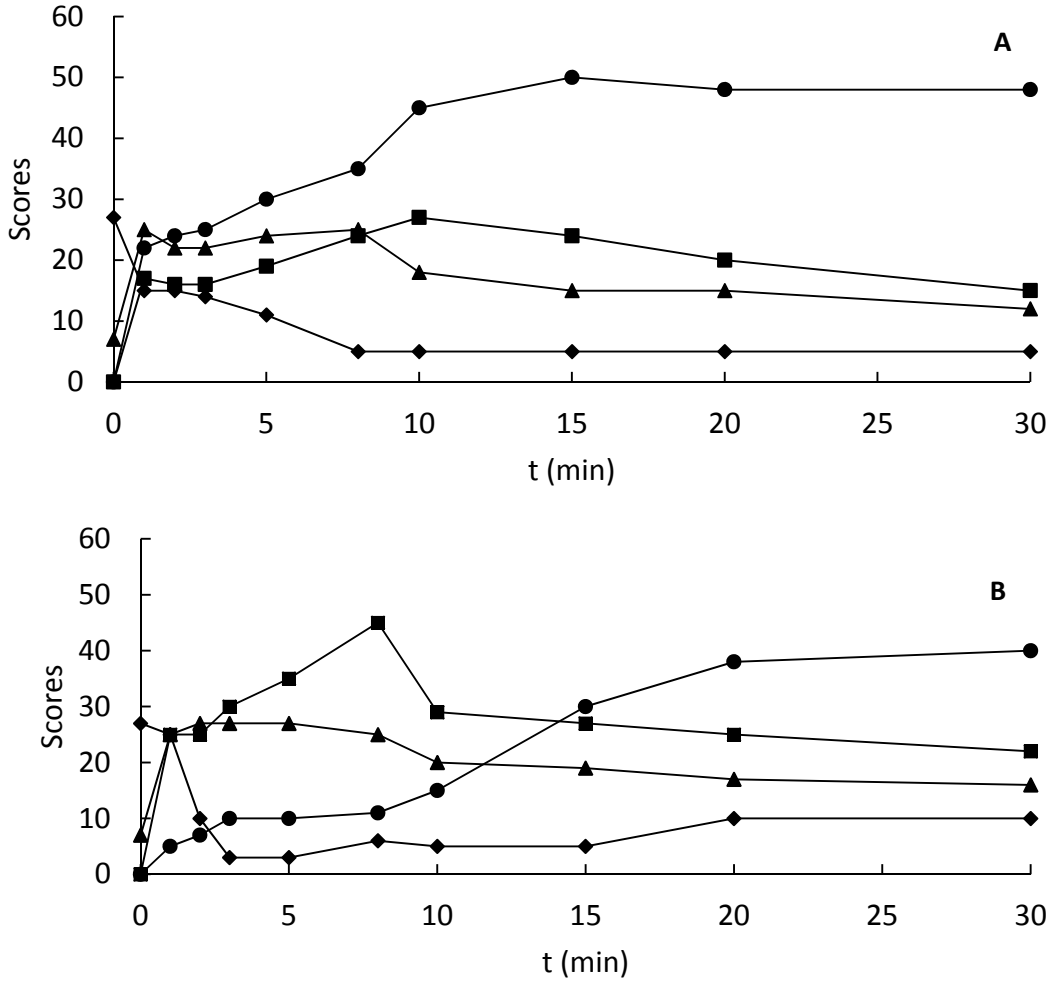

598 Figure 8. Time resolved plot of the scores reached by each component of the

599 PARAFAC analysis of the EEM matrixes obtained in the O_3 (A) and O_3/UVA-VIS (B)

600 treatment of a mixture of eight phenolic compounds The components are represented

601 by: C1 (●), C2(■), C3 (▲) and C4 (♦)

602